UDC 519.61:624.074.4
Original scientific paper
Received: 10.10.2000.

Model for static analyses of concrete shells

Jure Radnić[(1)], **Domagoj Matešan**[(2)] and **Alen Harapin**[(1)]
[(1)]University of Split, Faculty of Civil Engineering, Matice hrvatske 15, 21000 Split, CROATIA
e-mail: alen.harapin@gradst.hr
[(2)]Civil Engineering Institute of Croatia - Zagreb, Business Center Split, Matice hrvatske 15, 21000 Split, CROATIA
e-mail: domagoj.matesan@st.igh.hr

SUMMARY

The paper presents the model and the respective developed software for the static analysis of concrete plates and shells exposed to transient static loads by the finite element method (FEM). A degenerated shell element without membrane and shear "locking" has been employed. The model simulates the influence of material and geometric system nonlinearity. It is possible to include the dominant non-linear effects of reinforced concrete: the development of concrete cracks in tension and yielding of the concrete in compression, the changes in the tensile and shear stiffness of concrete and the nonlinear behaviour of the reinforcement. The influence of the change in the structure geometry is dealt with by using an updated Lagrangian coordinate system. The solved example illustrates the reliability of the model and some possibilities of the application of the model and of the SALJ computer program.

Key words*: concrete plates, concrete shells, transient static loads, degenerated shell element, material and geometric nonlinearity.*

1. INTRODUCTION

This paper presents a numerical model for the analysis of reinforced concrete shells subjected to transient static loads by the finite element method (FEM). The adopted degenerated shell finite element [1] eliminates the negative effect of the so-called shear and membrane "lockings". The 8 and 9 node elements of a curved shell with a layered material model across the shell thickness have been used.

The model is relatively simple and at the same time it includes the dominant nonlinear effects of the reinforced structures behaviour, such as:

- concrete yielding under compression,
- cracks development in concrete under tension,
- cracks opening and closing,
- tensile stiffness of cracked concrete,
- shear stiffness of cracked concrete,
- nonlinear behaviour of the reinforcement.

Concrete properties can vary for each layer of the shell. The reinforcement is modelled as a special layer of a respective thickness, with the strength and stiffness in the direction of the bars.

The use of the updated Lagrangian coordinates includes the influence of the change in the structure geometry. The coordinates of the system nodes are updated in each iterative step of solution seeking and the new displacement-strain relation is established.

The adopted numerical model is similar to Figueiras's model [2], with improvements which mainly refer to: (i) inclusion of a more precise and efficient degenerated shell element without the effect of the shear and membrane "lockings", (ii) more adequate simulation of the tensile stiffness of cracked concrete and (iii) better simulation of shear stiffness of cracked concrete.

The accuracy of the presented model and the developed SALJ computation program were verified by analysing one example for which there are already known experimental and numerical results.

2. ASSUMED DEGENERATED SHELL ELEMENT

Since reduced and selective integrations result in zero energetic modes, various authors have attempted to develop different alternative approaches to avoiding the problem of "lockings" [3-10]. The approach used in this paper is the substitution shear field approach, originally introduced by Bathe and Dvorkin [5] and later generalised by Huang [11].

The applied degenerated shell element [1] was developed by using:

- Assumed transverse shear strains expressed in the natural coordinate system [12];
- Assumed membrane strains expressed in the orthogonal curvilinear coordinate system [11].

This element has no problems related to "locking" and mechanism occurrence. The element is described in detail in Ref. [1].

3. MATERIAL MODELLING

3.1 Concrete modelling

A rather simple concrete model has been used in this paper [13-15], intended for everyday engineering practice, based on the basic concrete parameters (uniaxial compressive and tensile strength, the modulus of elasticity and Poisson coefficient) which should be known for other purposes anyway.

The graphical presentation of the adopted concrete model is presented in Figure 1. Subsequently, concrete modelling in tension and in compression is presented separately.

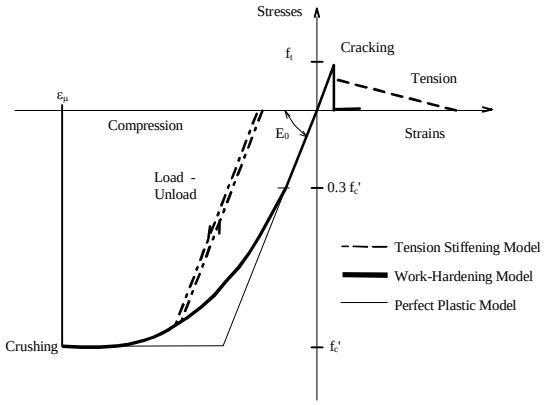

(i) One – dimensional representation

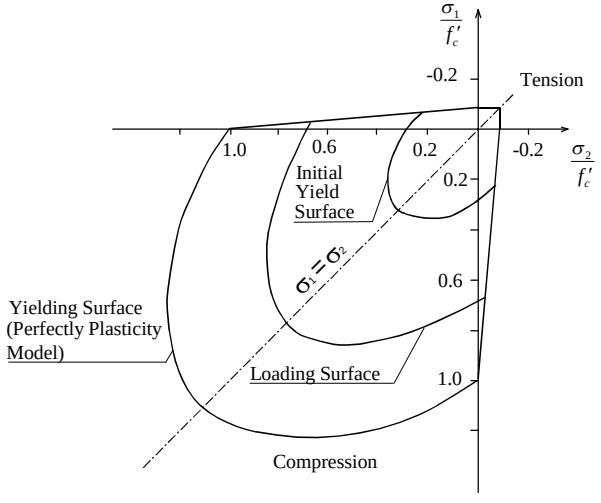

(ii) Two – dimensional representation

Fig. 1 Graphical review of concrete model

3.1.1 Modelling of concrete under tension

The graphic interpretation of the concrete model under tension is presented in detail in Figure 2. Linear-elastic concrete behaviour has been assumed until its tensile strength is reached. Cracks in concrete are assumed to appear only in planes perpendicular to the shell midsurface. Actually, it is considered that each concrete layer across the shell thickness is in the state of plane stress and that the cracks development is monitored for this state [13]. It is also assumed that even after cracking the concrete remains as a continuum. A model of the so-called smeared cracks has been used. It has been adopted that after the occurrence of the first crack, its position and direction do not change after subsequent changes of loading. Hence, the so-called model of fixed orthogonal cracks has been used. After the occurrence of cracks concrete becomes anisotropic, and the cracks directions define the main anisotropy directions. Both, partial and complete crack closings at unloading have been modelled as well as new opening of the previously developed cracks under repeated loading. The contribution of the uncracked concrete stiffness between cracks was simulated by gradually decreasing the component of tensile stress perpendicular to the crack plane. Figure 2 also illustrates the behaviour under unloading and reloading. If the crack is closed, i.e. when strain perpendicular to the crack plane is negative, the compressive stresses along the plane can be transferred in the same way as in homogeneous concrete. After repeated opening of the previously closed crack, it is necessary to take into account the previously decreased tensile stiffness, i.e. for repeated loads E is taken as in Figure 2.

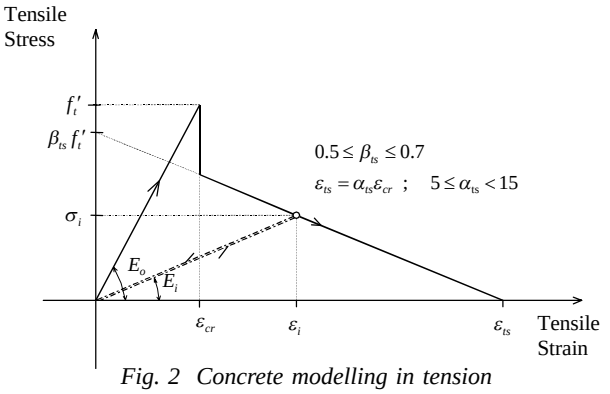

Fig. 2 Concrete modelling in tension

The shear stiffness of cracked concrete was simulated as in Figure 3. In other words, such a model has been adopted where the shear modulus of cracked concrete is taken as the function of the strain normal to the crack plane.

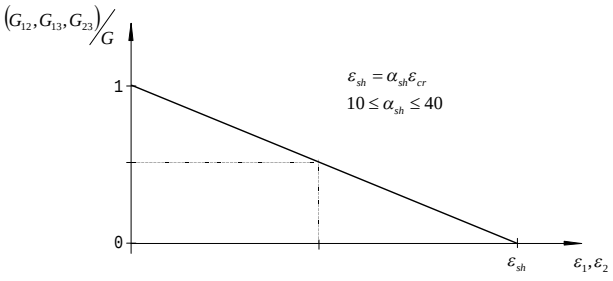

Fig. 3 Reduction of concrete shear modulus in cracking zones

3.1.2 Modelling of concrete under compression

Concrete modelling under compression is graphically presented in Figure 1. The compressive concrete behaviour was described using the flow theory of plasticity, for which it was necessary to define: the yielding condition, the flow rule and the hardening rule as well the crushing condition.

The yielding condition was defined by [2]:

$$f(\sigma) = \{0.355\sigma_0(\sigma_x + \sigma_y) + 1.355\left[(\sigma_x^2 + \sigma_y^2 - \sigma_x\sigma_y) + 3(\tau_{xy}^2 + \tau_{yz}^2 + \tau_{zx}^2)\right]^{\frac{1}{2}}\} = \sigma_0 \quad (1)$$

For the model with a completely plastic behaviour, σ_0 was taken as limit stress f_c' from the uniaxial compressive test. The so-called associated flow rule was used, i.e. it was assumed that the plastic strain vector is perpendicular to the yielding surface. The concept of effective stress and effective plastic strain was adopted to define the hardening rule. In unloading conditions, a linear behaviour was used with the initial modulus of elasticity of concrete. The crushing condition under compression was defined by the strain invariants, analogous to Eq. (1).

3.2 Reinforcement modelling

The method of reinforcement modelling is graphically presented in Figure 4, and the adopted stress-strain relationship for steel is presented in Figure 5.

The reinforcement bars are modelled as separate steel layers of equivalent (normalised) thickness ($A_{a\xi}$) at the respective (normalized) distance (ξ_a) from the central shell plane. The stresses can occur only in the bars direction. It was assumed that the concrete and reinforcement displacements were entirely compatible.

A bi-linear stress-strain relation was used to describe the steel behaviour, both in compression and in tension. For unloading conditions, a linear behaviour with the initial modulus of elasticity was assumed. The bars collapse occurs when the strain in their direction exceeds the limit value ε_{au}.

4. THE SOLUTION PROCEDURE

The known displacements $\boldsymbol{d}^n$, stresses $\boldsymbol{\sigma}^n$ and unbalanced nodal forces $\boldsymbol{\psi}_n$ from the previous (n) load increment are used. External current nodal forces are computed by:

$$\boldsymbol{\phi}_0^{n+1} = \boldsymbol{\phi}^n + \Delta\boldsymbol{R}^{n+1} \quad (2)$$

where $\boldsymbol{\psi}^n$ is residual forces at the end of the preceding load increment, and $\Delta\boldsymbol{R}^{n+1}$ is the current ($n+1$) load increment. The iterative process is given in Table 1.

5. NUMERICAL EXAMPLE

A parabolic cylindrical shell with a varying thickness was analysed, with a uniformly distributed load, which had been experimentally studied by Hedgren [16]. The shell was supported at two edges by a diaphragm, while the remaining two edges remained free. The shell geometry, data on the reinforcement and discretization by finite elements are presented in Figure 6. More detailed data on the geometry and reinforcement can be found in Ref. [16]. The analysis included only one fourth of the shell due to the problem symmetry. The shell was simulated across its thickness with 8 concrete layers. The reinforcement is non-uniformly distributed, i.e. concentration is more intense along the free edges. The shell is freely supported at the diaphragm, with free displacement in the direction of the x axis and rotation

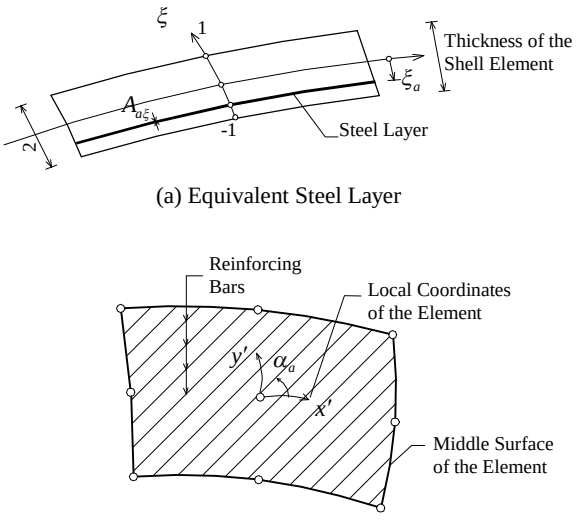

(a) Equivalent Steel Layer

(b) Spacing of Bars

Fig. 4 Modelling of reinforcement

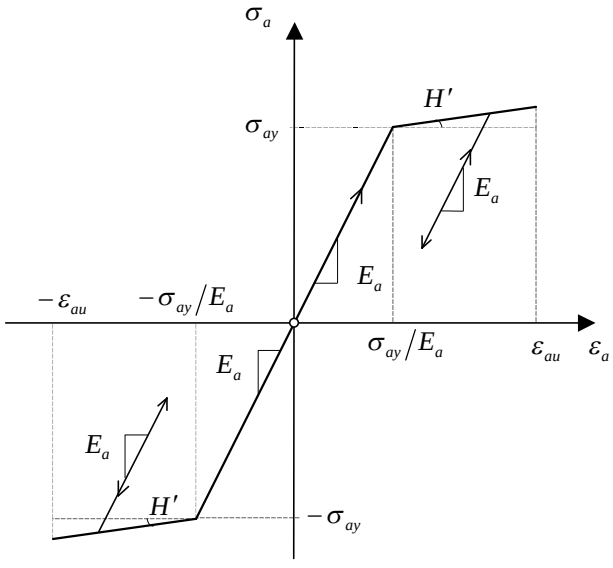

Fig. 5 Stress-strain relation for steel

angle around the *y* axis. The material parameters adopted for the numerical analysis are presented in Tables 2. The shell load is given by the ratio between the observed load (*P*) and the design load (P_{pr}=0,358 N/cm^2).

Some computational results are presented in Figures 7 and 8.

It is evident from the presented figures that the numerical results obtained by the SALJ program are almost completely in agreement with the results obtained by experiment [16], and with numerical results obtained by Figueiras [2]. Furthermore, it should be noted that the presented model is similar to Figueiras's model, with improvements listed in Section 1.

Table 1. The iterative process of the problem solution

(i) The stiffness matrix $\boldsymbol{K}$ *is updated or not, according to the adopted solution algorithm.*
(ii) The incremental displacements $\Delta\boldsymbol{d}_{i+1}$ *are evaluated from the equilibrium equation:* $$\Delta\boldsymbol{d}_{i+1} = -\boldsymbol{K}^{-1}\boldsymbol{\psi}_i$$ *where* $\boldsymbol{\psi}_i$ *are the unbalanced nodal forces from the previous iteration. The total displacement vector* $\boldsymbol{d}_{i+1}$ *is then updated by:* $$\boldsymbol{d}_{i+1} = \boldsymbol{d}_i + \Delta\boldsymbol{d}_{i+1}$$
(iii) The incremental strains $\Delta\boldsymbol{\varepsilon}_{i+1}$ *and the total strains* $\boldsymbol{\varepsilon}_{i+1}$ *are evaluated:* $$\Delta\boldsymbol{\varepsilon}_{i+1} = \boldsymbol{B}\Delta\boldsymbol{d}_{i+1}$$ $$\boldsymbol{\varepsilon}_{i+1} = \boldsymbol{\varepsilon}_i + \Delta\boldsymbol{\varepsilon}_{i+1}$$ *where* $\boldsymbol{B}$ *includes large displacements.*
(iv) The incremental stresses $\Delta\boldsymbol{\sigma}_{i+1}$ *and the total stresses* $\boldsymbol{\sigma}_{i+1}$ *are calculated:* $$\Delta\boldsymbol{\sigma}_{i+1} = \boldsymbol{D}\Delta\boldsymbol{\varepsilon}_{i+1}$$ $$\boldsymbol{\sigma}_{i+1} = \boldsymbol{\sigma}_i + \Delta\boldsymbol{\sigma}_{i+1}$$ *where* $\boldsymbol{D}$ *is the elasticity matrix taken as:* • *Either the elastic matrix for uncracked concrete or the corresponding matrix for cracked concrete for concrete layers* • *The elastic matrix for reinforcement steel layers*
(v) The stresses are corrected according to the material constitutive equations: • *Concrete layers* - *Using the total stresses* $\boldsymbol{\sigma}_{i+1}$ *the maximum principal stresses* σ_1, σ_2 *acting in the shell plane are calculated, as well as the angle of principal stresses* - *If* $\sigma_1 > f_t'$ ($\sigma_2 > f_t'$), *or, if the concrete is already cracked, the stresses are updated according to the adopted model of tension stiffening of cracked concrete.* - *The effective stress* $\overline{\sigma}$ *is calculated (according to the yield function) using* $\boldsymbol{\sigma}_{i+1}$ *or the updated stresses from the previous step.* - *If* $\overline{\sigma}$ *is greater than the initial yield stress or if the layers have already yielded, the stresses are corrected according to the adopted elasto-plastic behaviour.* • *Steel layers* - *Total stresses* $\sigma_{a_{i+1}}$ *and total strains* $\varepsilon_{a_{i+1}}$ *in the reinforcement bars direction are calculated* - *Stresses are updated according to Figure 5. If* $\varepsilon_{a_{i+1}} > \varepsilon_{au}$, *the bar is consider being broken.*
(vi) Equivalent nodal forces $\boldsymbol{p}_{i+1}$ *are calculated using the stress integration, as:* $$\boldsymbol{p}_{i+1} = \int_V \boldsymbol{B}^T \boldsymbol{\sigma}_{i+1} dV$$ *where* $\boldsymbol{\sigma}_{i+1}$ *are the total corrected stresses according to the constitutive equations (material law).*
(vii) The out of balance forces $\boldsymbol{\psi}_{i+1}$ *are calculated:* $\boldsymbol{\psi}_{i+1} = \boldsymbol{R}_{i+1} - \boldsymbol{p}_{i+1}$
(viii) The convergence of the process is checked - *If convergence criterion has been achieved, proceed to the next load increment.* - *If the convergence criterion has not been satisfied restart from step (i).*

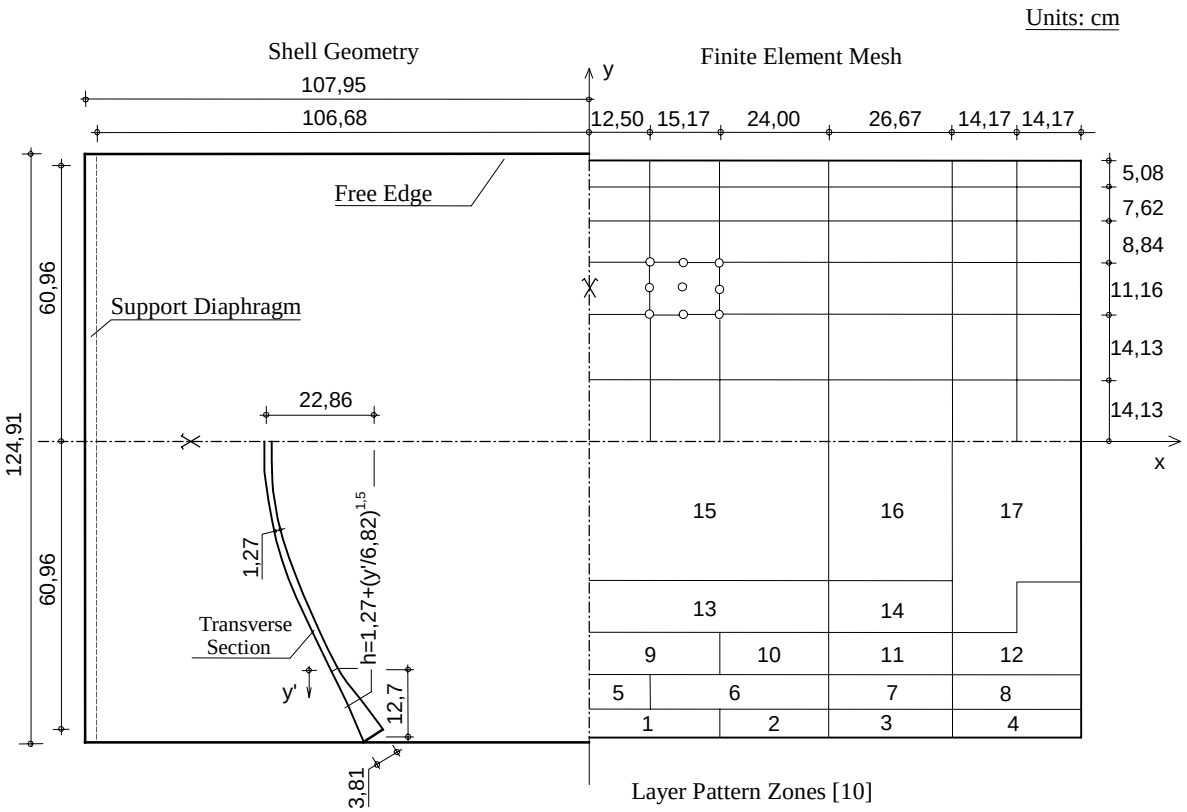

Fig. 6 Geometry and finite element idealisation for a parabolic cylindrical shell [16]

Table 2. Material parameters

Concrete		*Steel*		
Elasticity modulus	$E_c = 2069\ kN/cm^2$	*Elasticity modulus*		$E_a = 20000\ kN/cm^2$
Poisson's ratio	$\nu = 0.145$	*Poisson's ratio*		$H' = 4000\ kN/cm^2$
Ultimate compressive strength	$f_c' = 3.02\ kN/cm^2$	*Yield strain*		0.01
Ultimate tensile strength	$f_t' = 0.48\ kN/cm^2$	*#3*	*Yield stress*	$\sigma_y = 25.29\ kN/cm^2$
Crushing strain	$\varepsilon_{cu} = 0.0035$		*Ultimate stress*	$f_a = 36.42\ kN/cm^2$
Tensile stiffness parameters	$\varepsilon_m = 0.5$	*#4*	*Yield stress*	$\sigma_y = 21.91\ kN/cm^2$
	$\varepsilon_{ts} = 0.002$		*Ultimate stress*	$f_a = 34.49\ kN/cm^2$
Shear stiffness parameter	$\varepsilon_{sh} = 0.002$	*#9*	*Yield stress*	$\sigma_y = 30.66\ kN/cm^2$
			Ultimate stress	$f_a = 42.00\ kN/cm^2$

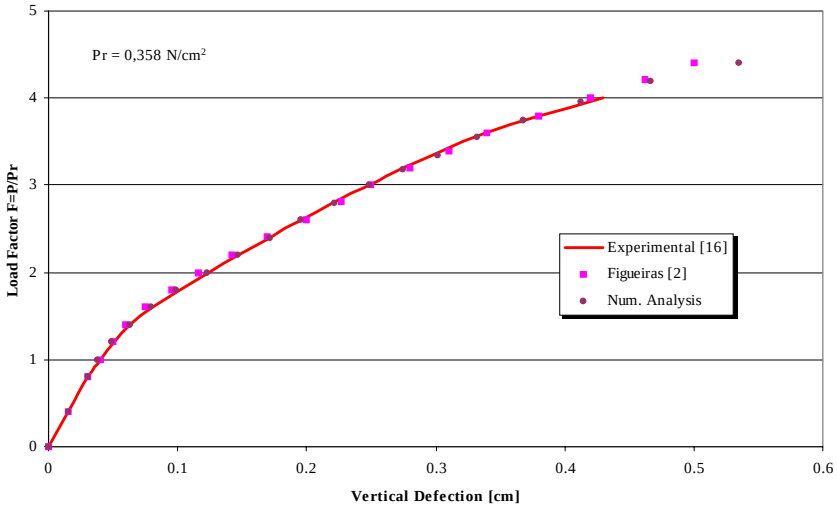

Fig. 7 Vertical deflection of the free edge

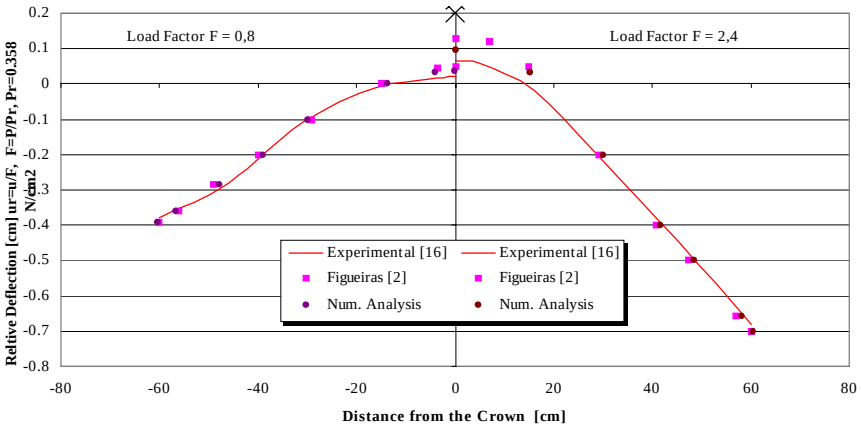

Fig. 8 Vertical deflection of the transverse section at mid-span

6. CONCLUSION

The presented model for the analysis of concrete shells exposed to instantaneous static loading includes the dominant non-linear material and geometry effects of the structure behaviour. The model is based upon the basic concrete and reinforcement parameters and is primarily intended for application in actual engineering practice. Presented example as well as others solved examples illustrate the accuracy and reliability of the proposed model and developed computational program SALJ.

REFERENCES

[1] H.C. Huang, *Static and Dynamic Analysis of Plates and Shells*, Springer-Verlag, 1989.

[2] J.A. Figueiras, Ultimate load analysis of anisotropic and reinforced concrete plates and shells, Ph.D. Thesis, University College of Swansea, C/Ph/72/83, 1983.

[3] K.J. Bathe and E.N. Dvorkin, A four-node plate bending element based on Mindlin/Reissner plate theory and a mixed interpolation, *Int. J. Numer. Meth. Engng.*, Vol. 21, pp. 367-383, 1985.

[4] T. Belytschko, J.S.J. Ong and W.K. Liu, A consistent control of spurious single modes in the 9-node Lagrange element for the Laplace and Mindlin plate equations, *Comp. Meth. App. Mech. Engng.*, Vol. 44, pp. 269-295, 1984.

[5] E.N. Dvorkin and K.J. Bathe, A continuum mechanics based four-node shell element for general non-linear analysis, *Engng. Comp.*, Vol. 1, pp. 77-88, 1984.

[6] I. Fried, Triangular nine-degrees-of-freedom, C(0) plate bending element of quadratic accuracy, *Q. Appl. Mech.*, Vol. 31, pp. 303-312, 1973.

[7] I. Fried, Shear in C(0) and C(1) bending finite elements, *J. Solids Struct.*, Vol. 9, pp. 449-460, 1973.

[8] I. Fried, Residual energy balancing technique in the generation of plate bending element, *Comp. Struct.*, Vol. 4, pp. 771-778, 1974.

[9] T.J.R. Hughes and W.K. Liu, Nonlinear finite element analysis of shells: Parts I and II: three dimensional and two dimensional shells, *Comp. Meth. Appl. Mech. Engng.*, Vol. 26, pp. 331-362, & Vol. 27, pp. 167-181, 1981.

[10] T.J.R. Hughes and T.E. Tezduyar, Finite elements based upon Mindlin plate theory with particular reference to the four-node bilinear isoparametric element, *Trans. ASME E.: J. Appl. Mech.*, Vol. 48, pp. 587-596, 1981.

[11] H.C. Huang and E. Hinton, A new nine node degenerated shell element with enhanced membrane and shear interpolation, *Int. J. Num. Meth. Eng.*, Vol. 22, pp. 73-92, 1986.

[12] H.C. Huang and E. Hinton, A nine node Lagrangian Mindlin plate element with enhanced shear interpolation, *Engineering Computations*, Vol. 1, pp. 369-379, 1984.

[13] D. Matešan, Nonlinear analysis of concrete shells, M.Sc. Thesis, Faculty of Civil Engineering, University of Split, Split, 2000. (in Croatian).

[14] J. Radni}, Static and dynamic analysis of gravity dams, *Gra|evinar*, Vol. 45, No. 2, pp. 63-73, 1993. (in Croatian)

[15] J. Radni} and F. Damjani}, Numerical model for static and dynamic analysis of reinforced structures, *Izgradnja*, Vol. 10, pp. 5-14, 1989. (in Croatian)

[16] A.W. Hedgren and D.P. Billington, Mortar model test on a cylindrical shell of varying curvature and thickness, *ACI Journal*, 1967.

[17] S. Ahmad, Curved finite elements in the analysis of solid, shell and plate, Ph.D. Thesis, University College of Swansea, C/PH/7/69, 1969.

[18] S. Ahmad, B.M. Iron and O.C. Zienkiewicz, Analysis of thick and shell structures by curved finite elements, *Int. J. Numer. Meth. Engng.*, Vol. 2, pp. 419-451, 1970.

[19] P.G. Bergan and I. Holand, Nonlinear finite element analysis of concrete structures, *Comp. Meth. in App. Mech. and Eng.*, Vol. 17/18, pp. 443-467, 1979.

[20] L. Cedolin, Y.R.J. Crutzen and S. Deipoli, Triaxial stress-strain relationship for concrete, *ASCE J. of the Eng. Mech. Div.*, Vol. 103, No. EM3, pp. 423-439, 1977.

[21] H. Duddeck, G. Griebenow and G. Shaper, Material and time dependent nonlinear behaviour of cracked reinforced concrete slabs, In: Nonlinear Behaviour of Reinforced Concrete Spatial Structures, Vol.1., Preliminary Report IASS Symposium held in Darmstadt, Eds. G. Mehlhorn, H. Ruhle and W. Zerna, Werner-Verlag, Dusseldorf, pp. 101-113, 1978.

[22] J.A. Figueiras and D.R.J. Owen, Analysis of elasto-plastic and geometrically non-linear anisotropic plates and shells, In: Finite Element Software for Plates and Shells, Eds. E. Hinton and D.R.J. Owen, Pineridge Press, 1984.

[23] R.I. Gilbert and R.F. Warner, Tension stiffening in reinforced concrete slabs, *ASCE Journal of the Structural Division*, Vol. 104, No. ST12, pp. 1885-1900, 1978.

[24] F.R. Hand, D.A. Pecknold and W.C. Schnobrich, Nonlinear layered analysis of RC plates and shells, *ASCE Journal of the Structural Division*, Vol. 99, No.ST7, pp. 1491-1505, 1973.

[25] H.C. Huang and E. Hinton, Elasto-plastic and geometrically nonlinear analysis of plates and shells using a new nine node element, In: Proceedings of Symposium Finite Element Methods for Nonlinear Problems, Vol. 1, pp. 3-1-3-15, Trondheim, Norway, 1985.

[26] H.B. Kupfer and K.H. Gerstle, Behaviour of concrete under biaxial stresses, *ASCE Journal of the Eng. Mech. Div.*, Vol. 99, No. EM4, pp. 853-866, 1973.

[27] C.S. Lin and A.C. Scordelis, Nonlinear analysis of RC shells of general form, *ASCE Journal of the Structural Division*, Vol. 101, No. ST3, pp. 523-538, 1975.

[28] R.D. Mindlin, Influence of rotatory inertia and shear in flexural motion of isotropic, elastic plates, *J. Appl. Mech.*, Vol. 18, pp. 1031-1036, 1951.

[29] E. Reissner, The effect of transverse shear deformation on bending of elastic plate, *J. Appl. Mech.*, Vol. 12, pp. 69-76, 1945.

[30] S.P. Timoshenko and S. Woinowsky-Krieger, *Theory of plates and shells*, 2nd edn., McGraw-Hill, New York, 1961.

MODEL ZA STATI^KE ANALIZE BETONSKIH LJUSKI

SA@ETAK

Izlo`en je model i razvijen odgovaraju}i software za stati~ku analizu betonskih plo~a i ljuski, optere}enih kratkotrajnim stati~kim optere}enjem, s pomo}u metode kona~nih elemenata. Uporabljen je degenerirani element ljuske, kod kojega su eliminirani utjecaji tzv. posmi~nog i membranskog "locking-a". Model simulira utjecaj materijalne i geometrijske nelinearnosti sustava. Mogu}e je uklju~iti dominantne nelinearne efekte armiranog betona: razvoj pukotina betona u vlaku i te~enje u tlaku, promjenu vla~ne i posmi~ne krutosti betona, te nelinearno ponašanje armature. Utjecaj promjene geometrije konstrukcije obuhva}en je preko pomi~nog Lagrange-ovog koordinatnog sustava. Koristi se op}i degenerirani element ljuske, oslobo|en membranskog i posmi~nog "locking-a". Riješeni primjeri ilustriraju pouzdanost i neke mogu}nosti primjene modela i prora~unskog programa SALJ.

***Klju~ne rije~i**: betonske plo~e, betonske ljuske, kratkotrajno stati~ko optere}enje, degenerirani element ljuske, materijalna i geometrijska nelinearnost.*